Electron thermalization ranges and free-ion yields in dielectric fluids: Effects of density and molecular shape

Norman Gee and Gordon R. Freeman
Department of Chemistry, University of Alberta, Edmonton, Alberta T6G 2G2, Canada
(Received 18 April 1983)

Secondary-electron thermalization ranges b_{GP} and free-ion yields G_{fi}^{E} have been measured in the coexistence vapor and liquid of spherelike (methane) and nonspherelike (ethane) molecules at densities $0.14 \lesssim d/d_c \lesssim 2.8$, where d_c is the density of the critical fluid. The density-normalized range $b_{GP}d$ at low d is 5.5×10^{-6} kg/m^2 in both compounds. In the dense gas at $d/d_c \gtrsim 0.3$, $b_{GP}d$ increases slightly; the effective cross section for epithermal electron scattering is lessened. The large density fluctuations at these conditions, which cause quasilocalization of thermal electrons, appear to affect epithermal electrons in an opposite fashion. At $d/d_c > 1.0$, conduction-band formation lifts $b_{GP}d$ in liquid methane to ~ 4 times the value in liquid ethane. The density effect is in the same direction as, but less marked than, that for thermal electrons. At $d/d_c = 2.5$, b_{GP} in methane is 1.2 times *larger* than at $d/d_c = 1$, but the mobility μ of thermal electrons is 15 times larger than at $d/d_c = 1$. In ethane at $d/d_c = 2.5$, b_{GP} is 3.4 times and μ is 33 times *smaller* than at $d/d_c = 1$. The degree of sphericity of the molecules greatly affects electron energy loss and localization interactions.

I. INTRODUCTION

Ions and electrons that are collectable at electrodes in a dense fluid are called "free ions";[1] they diffuse independently and not in correlated pairs. The generation of free ions in a dense fluid by ionization of a molecule requires that an electron be ejected from the molecule with sufficient excess kinetic energy to escape the field of its sibling cation in spite of energy-loss collisions with surrounding molecules. The electron eventually loses its excess kinetic energy in these collisions and becomes thermalized at some distance b from the sibling ion. Whether the ion and electron then undergo geminate recombination depends on the magnitudes of b and the dielectric constant ϵ of the intervening fluid. The magnitude of b depends on the fluid density and on the physical shape[2-10] and polarity[11,12] of the molecules. The density effect is due mainly to the number density of scatterers, which inversely affects the projectile's mean free path. At high densities, collective effects at low energies alter the nature of the scatterers. The major portion of the thermalization distance b in liquids is attained while the electron is at subvibrational energies,[13-16] skittering along in the conduction band.[17-20] (The term "skittering" refers to the much gentler and less frequent collisions that an electron undergoes inside the band than it did while above the band.)

The effect of molecular shape is illustrated as follows. Electrons in liquids of spherelike molecules have greater thermalization distances and higher mobilities than they do in liquids of nonspherelike molecules.[14,15] The conduction band which is formed by overlap of the lowest unoccupied orbitals has a less undulating lower surface in fluids of spherelike molecules than in fluids of nonspherelike molecules. Electrons are therefore less strongly scattered and they less readily form localized states in the former than in the latter.

In a low-density gas the molecules are too far apart for a conduction band to form. The thermalization distance is inversely proportional to the density d. On going from the gas to the liquid, the density-normalized distance bd should, therefore, increase as the conduction-band forms. The increase should be greater when the molecules are spherelike than when they are nonspherelike.

The most spherelike hydrocarbon molecule is methane, CH_4. The simplest nonspherelike hydrocarbon molecule is ethane, H_3CCH_3. The thermalization distance in liquid methane is about five times larger than that in liquid ethane.[21-23] The present article reports the variations of the density-normalized thermalization distances in methane and ethane as the densities are reduced from those of the normal liquids to those of the vapors. The variation of bd with d is quite different in methane than in ethane.

II. EXPERIMENTAL

A. Material

The methane was either Matheson Research Purity (99.99%) or Linde Ultrahigh Purity (99.97%). The ethane was Phillips Research Grade (99.97%). About 30 g of the required compound was transferred to a grease-free vacuum line through flexible stainless-steel tubing that was welded to a Kovar-glass seal. Further purification was accomplished by treatment with Davison 3A molecular sieves, degassing by distillation under vacuum, and prolonged contact with several fresh potassium mirrors.[24,25]

B. Methods

The conductance cells were similar to the thick-walled cells described in Ref. 19. The one used for gas-phase measurements had sidearms pointing upwards compared to the one in Fig. 1 of Ref. 19. The electrode separation was 3.2 mm and the effective collector area was 2.5 cm^2.

The temperature control system is described in Refs. 18 and 24. Low temperatures were attained with cold nitrogen gas and high temperatures with air from a heat gun.

Free-ion yields $G_{\rm fi}^{E}$ were measured by sweeping radiation-produced charges from the cell by an electric field E and integrating them.[14] A 0.10- or 1.0-μs pulse of 1.7-MeV x rays delivered (~ 0.6 or 6)$\times 10^{11}$ eV/g to the sample. The center of the conductance cell was 34 cm from the gold x-ray target. The calibration constant was $\sim 5\times 10^{9}$ eV/g absorbed in the sample for each nC deposited by the Van de Graaff electron beam on the target.

Liquid-phase dosimetry was done through a three-step sequence. The dose delivered by each pulse was monitored by measuring the charge deposited on the gold target by the pulse of 1.7-MeV electrons from the Van de Graaff accelerator. This pulse monitor was calibrated by measuring the thermoluminescence generated by LiF crystals after an accumulation of 10^{2}–10^{3} pulses.[22] The pulses for calibration were produced at a rate of only 4/s to allow complete recovery of the accelerator cathode charge between pulses. The LiF-crystal dosimeters were from Harshaw Nuclear Systems Co. (TLD-700) and the thermoluminescence measuring unit was a Harshaw Model 2000-A. The standard deviation of the readings from five crystals selected at random from a batch of 20 was 2–6%. The five crystals were stacked vertically, on edge, in a thin-walled ($\sim\frac{1}{2}$ mm) glass tube and placed between the electrodes of a dummy cell. The dummy cell had the same electrode and wall construction as the measurement cells. The liquid in the dummy cell was n-pentane. The thermoluminescent crystals were calibrated against the Fricke dosimeter[26] using a ^{60}Co γ-ray source. The crystals were irradiated in the dummy cell for 60–90 s ($\sim 3\times 10^{14}$ eV/g), while the Fricke solutions were irradiated at the same location for $\frac{1}{2}$–6 h. Conversion from dose in Fricke solutions to dose in hydrocarbons was calculated by way of the Bethe equation[26] using the appropriate electron densities and mean ionization potentials. The values of the latter were estimated[27] to be 69 eV for the Fricke solution, 45 eV for methane, 49 eV for ethane, and 85 eV for air. The mean energy of the secondary electrons was taken to be 10^{4} eV.

Dosimetry in the low-density gas phase was done by calibrating the pulse monitor against the ionization produced in air in the measuring cell. The average amount of energy absorbed per ionization in air at atmospheric pressure and ~ 300 K is 33.8 eV,[28,29] or $G_{\rm tot}=2.96$.

Application of the Fricke-LiF dosimetry in the above manner to energy absorption in air at 94 kPa and 295 K gave G(ionization)$=4.2$, which is 43% too large. The steel electrodes have an electron density twice that of the glass walls and seven times that of the Fricke solutions. Thus, the rate of energy absorption from the x rays was greater in the steel than in the glass or Fricke solution. More high-energy electrons would be ejected from the steel to ionize gas molecules than would be estimated from energy absorption in the Fricke solutions. Direct dosimetry with air in the conductance cell was therefore necessary. The transition in dose from air to Fricke values was assumed to vary linearly with electron density. The error in this assumption might be up to 15%; it will have only a small effect upon the conclusions about the effect of density on electron thermalization distances in methane and ethane.

As the applied field strength approaches zero, the yield of collected charges approaches zero due to the competing neutralization reaction of the randomly distributed ions and electrons. The collection efficiency is given by[30]

$$f = u^{-1}\ln(1+u)\,, \tag{1}$$

where u^{-1} is proportional to E. For a given drift distance and initial charge density, u^{-1} is proportional to the neutralization rate constant α and to the reciprocal of the collection time t_d^{-1}. In the present work the fields were high enough that homogeneous neutralization was negligible.

C. Physical properties

The densities and critical-fluid parameters are from Refs. 31–33. The dielectric constants were calculated from the Lorenz-Lorentz equation[34] using as bases the methane dielectric constants from Ref. 35 and the ethane refractive indices from Ref. 36. Reference parameters are listed in Table I.

III. RESULTS AND DISCUSSION

A. Method and scope

The sequence of events in the radiation-induced ionization of molecules M in a fluid may be represented as

$$M \sim\!\!\sim\!\!\sim\!\!\rightarrow [M^{+}+e^{-}]\,, \tag{2}$$

$$[M^{+}+e^{-}]\rightarrow M\,, \tag{3}$$

which represents geminate neutralization,

$$[M^{+}+e^{-}]\rightarrow M^{+}+e^{-}\,, \tag{4}$$

which represents free ion formation,

TABLE I. Physical properties (Refs. 31–36). Subscripts: c is the critical point, b is the normal boiling point, t is the triple point. ϵ_c is the dielectric constant.

	CH_4	C_2H_6
T_c (K)	190.6	305.5
d_c (kg/m^3)	162	203
n_c (10^{26} molecule/m^3)	60.9	40.6
P_c (MPa)	4.60	4.88
ϵ_c	1.23	1.25
T_b (K)	111.4	184.5
d_b (kg/m^3)	429	549
T_t (K)	90.7	89.9
d_t (kg/m^3)	453	659

$$M^+ \rightarrow \text{cathode}\,, \qquad e^- \rightarrow \text{anode}\,, \tag{5}$$

which represent the collection by field; and where the square brackets indicate that the Coulombic interaction between the ion and electron must be taken into consideration. The yield of reaction (2) is represented by G_{tot}, the number of ion-electron pairs initially formed per 100 eV of energy absorbed by the system. The corresponding yield of free ions collected by an applied electric field of strength E is represented by G_{fi}^E. Electron thermalization distances can be estimated from the ratio $G_{\text{fi}}^E/G_{\text{tot}}$.

Free-ion yields were measured at different fluid densities through the gas, critical, and liquid phases. Examples of data for methane and ethane are shown in Fig. 1. The yield tends to decrease with increasing density due to the decreasing thermalization distance and consequent increase in the amount of geminate neutralization.[11,37] At the lowest density, 12 kg/m^3 of methane (17 amagats), geminate neutralization was negligible and only the total ionization yield $G_{\text{tot}}=3.8$ was measured. The field dependence of the yields in methane at $d \geq 23$ kg/m^3 or ethane at $d \geq 28$ kg/m^3 (Fig. 1) indicates that geminate neutralization occurs at these densities.

The lowest density at which geminate neutralization is appreciable in the x-irradiated gases is $d/d_c \approx 0.1$. This is similar to the lower limit observed by free-ion yield measurements in ethene, propane, and carbon dioxide,[38] and by the density effect on radiolysis final-product yields in ammonia,[39] ethane,[40] propene,[41] and cyclohexane.[42]

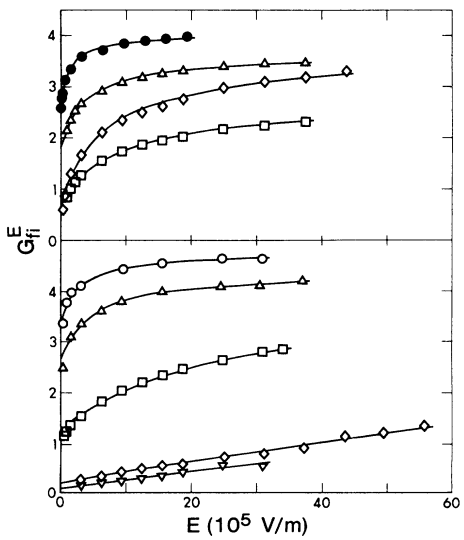

FIG. 1. Free-ion yields G_{fi}^E as functions of applied field strength E. Open symbols represent the averages of results from positive and negative applied voltages. Closed symbols represent results from negative voltages only. The temperatures (K) and densities (kg/m^3) were as follows. CH_4: ●, 158, 23; △, 173, 46; □, 192, 162$=d_c$; ◇, 91, 453 (liquid). C_2H_6: ○, 256, 28; △, 273, 46; □, 306, 203$=d_c$; ◇, 224, 503 (liquid); ▽, 166, 571. The solid curves were calculated from Eqs. (6)–(9) using parameter values from Table II.

B. Estimation of thermalization distances

In fluids irradiated with x rays or high-energy electrons about half of the ionizations of reaction (2) occur in spatially isolated events.[43] The events are separated by ~ 0.1 μm in a normal liquid and ~ 100 μm in a gas of density $\sim 10^{25}$ molecule/m^3. The other half of the ionizations occur in clusters of two or more, with relative probabilities that decrease with increasing number of ionizations per cluster. The initial configuration of such a cluster is that two or more approximately nearest-neighbor molecules are ionized within a period of $\sim 10^{-15}$ s. The electrons are ejected in random directions and become thermalized through scattering within $\sim 10^{-12}$ s at various distances from the positive ions. The average of many such spurs gives an isotropic distribution of thermalization distances described by an appropriate radial function.[44] In the jargon of radiation physics and chemistry, the reaction zone indicated by the square brackets in reaction (2) is called a *spur* and it may initially contain one or more ion-electron pairs.[45] A model based on a realistic distribution of ionizations per spur is complex and remains in a crude state.[44] However, in multipair spurs the multicharged core causes geminate neutralization to rapidly reduce the number of surviving pairs to one per spur. A reasonable, tractable model could therefore be based on spatially isolated ionizations (single pair spurs) with a value of G_{tot} somewhat lower than the true one. Such a model was originally put forward by Onsager[37] and has been extended[1,15] and improved.[46,47] The equations are as follows:

$$G_{\text{fi}}^E = G_{\text{tot}} \int_0^\infty F(y)\phi_{\text{fi}}^0[1+f(E,y,T)]dy\,, \tag{6}$$

where $F(y)dy$ is the fraction of electrons that have thermalization distances between y and $y+dy$, and ϕ_{fi}^0 is the probability that an electron with thermalization distance y escapes geminate neutralization (becomes a free ion due to random diffusion) in the absence of an external electric field;

$$\phi_{\text{fi}}^0 = \exp(-r_c/y)\,, \tag{7}$$

where $r_c = \xi^2/4\pi\epsilon_0\epsilon kT$ is the distance (m) at which the Coulombic attraction between the ion and electron equals the average thermal energy kT (J), ξ is the protonic charge (C), and ϵ_0 is the permittivity of vacuum. The function $f(E,y,T)$ describes the fractional enhancement of G_{fi}^E with increasing E,

$$f(E,y,T) = e^{-\beta y}\sum_{n=1}^{\infty}\frac{(\beta y)^n}{(n+1)!}\sum_{j=0}^{n-1}(n-j)\frac{(r_c/y)^{j+1}}{(j+1)!}\,, \tag{8}$$

where $\beta = \xi E/kT$, E is in V/m, and y is in m.

The form of the thermalization-distance distribution function $F(y)$ is not accurately known.[48–55] The two favored forms are exponential and Gaussian.[51] There seems to be no rational way of generating an exponential distribution in a scattering medium, but this function exaggerates the probability of small y values, which partially compensates for the neglect of the multicharged cores in

some of the spurs. The rapid collapse of the inner portions of multipair spurs leaves the pairs with the largest y value to participate in free-ion formation, so both the exponential and Gaussian functions require an extended tail that is an artifact of the single-pair spur model. The preferred function is a Gaussian with a power tail, designated Y_{GP} (Ref. 15):

$$F(y)=\begin{cases}0.96Y_G, & y<2.4b_{GP}\\ 0.96[Y_G+0.5(b_{GP}^2/y^3)], & y>2.4b_{GP}\end{cases} \quad (9)$$

where 0.96 is a normalization factor, $Y_G=(4y^2/\pi^{1/2}b_{GP}^3)\times\exp(-y^2/b_{GP}^2)$, and b_{GP} is the dispersion parameter and most probable value of the thermalization distance y. Equations (6)–(9) are fitted to experimental sets of (G_{fi}^E,E,T) data to obtain values of b_{GP} and G_{tot}.

C. DENSITY EFFECTS

Ionization yields were measured with both positive and negative applied voltages to detect possible effects of adventitious fields. The charge collected was normally independent of the sign of the applied voltage. Occasionally a set of G_{fi}^E values obtained with one sign would be up to 30% different from that obtained with applied voltages of the opposite sign, and the sets were discarded. In these cases the positive applied voltages usually registered ion yields that were too high, but the effect was not reproducible and seems to have had to do with the condition of the massive conductance cell (strain voltages in insulators?).

All of the results reported herein are averages of those obtained with positive and negative applied voltages, with the exception of methane at 12 and 23 kg/m^3 (Fig. 1). In those samples, positive applied voltages gave yields that were 12% and 9% higher than the rest of the set, so only the negative voltage results were used.

The value of G_{fi}^E increases monotonically with E in fluids with densities >20 kg/m^3 (Fig. 1). In ethane at a given E, the value of G_{fi}^E decreases monotonically with increasing density through the gas and liquid phases (Fig. 1). In methane, however, the value of G_{fi}^E at a given E decreases with increasing density through the gas phase and increases again on going to the liquid phase (Fig. 1).

The values of G_{tot} extracted from the results are nearly independent of density (Fig. 2). The lowest value in each compound occurs for the near-critical fluid and is believed to be an artifact. The large density fluctuations in the near-critical fluids might affect the nonhomogeneous kinetics of the system sufficiently to distort the G_{fi}^E against E curve away from Eq. (6)–(9); the factors most seriously affected would probably be the $F(y)$ distribution and the microscopic dielectric constant.

The value of G_{tot} is probably somewhat larger in the liquid than in the gas.[56,57] The increase is not evident in Fig. 2, probably due to the rapid geminate neutralization in the centers of multipair spurs mentioned earlier.

In the highest density liquid-ethane sample, $d=571$ kg/m^3, G_{fi}^E varies linearly with E over the range measured (Fig. 1). The curve-fitting procedure then becomes insensitive to the value of G_{tot} above a certain minimum, which in this case is 3.0. Larger values of G_{tot} simply require lower values of b_{GP} to fit the straight line. This flexibility is indicated by the error bars in Fig. 2.

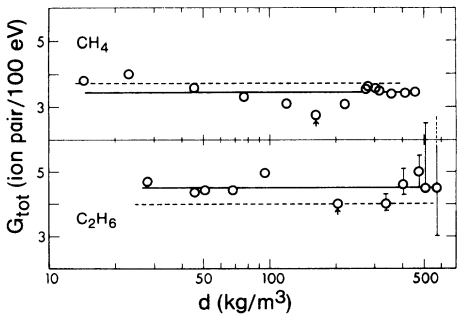

FIG. 2. Total ionization yields estimated by fitting Eqs. (6)–(9) to results such as those in Fig. 1. —, average value; — — —, average of values reported (Refs. 28 and 29) for the low-density gases. The arrows indicate the densities d_c of the critical fluids. The liquids and gases at $d\neq d_c$ are coexistence fluids.

The ratio G_{fi}^0/G_{tot} is the mean probability that an ion-electron pair will escape geminate neutralization in the absence of an applied electric field. The ratio in ethane decreases gently with increasing density in the gas phase and through the critical region into the low-density liquid, then plunges rapidly at $d/d_c>1.7$ (Fig. 3). The value obtained from electron-scavenging yield measurements[58] is consistent with the present work. The ratio in gaseous methane behaves similarly to that in ethane, but at $d>d_c$ the behavior is very different. In liquid methane the ratio increases, passes through a maximum at $d/d_c=1.4$, and decreases upon further increase of the density (Fig. 3).

The density-normalized thermalization distances $b_{GP}d$ are similar in the two gases. In Fig. 4, $b_{GP}d$ is plotted against the density normalized to the critical fluid density, d/d_c. The normalized thermalization distances increase

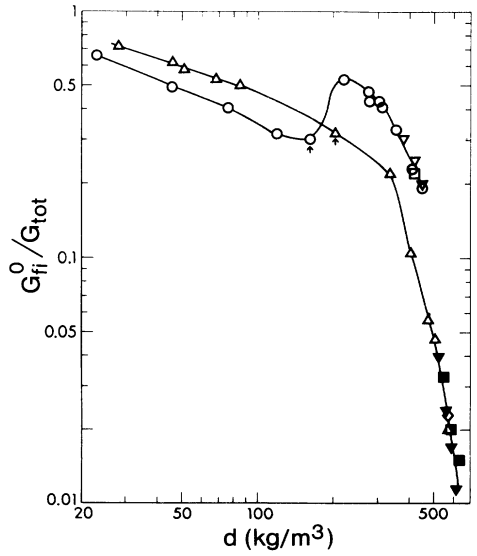

FIG. 3. Ratio of the free-ion yield at $E=0$ to the total ionization yield as a function of fluid density. CH_4: ○, present work; □, Ref. 22; ▽, Ref. 23. C_2H_6: △, present work; ■, Ref. 22; ▼, Ref. 23; ◇, Ref. 58, electron scavenging by nitrous oxide. The arrrows indicate the critical density d_c.

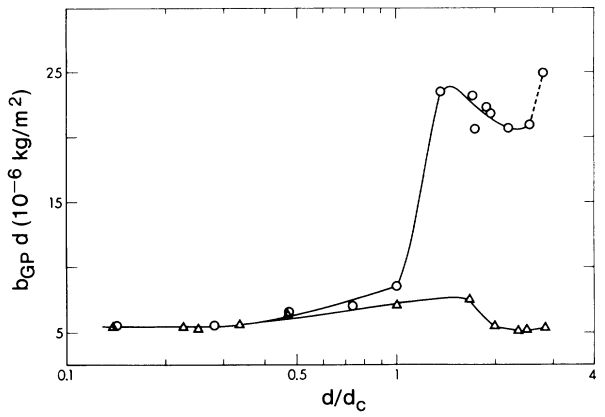

FIG. 4. Thermalization distance normalized for density $b_{GP}d$, plotted against the density normalized to the critical density, d/d_c. ○, methane; △, ethane. The highest point for methane might correspond to a partially frozen sample.

gently in the dense gases at $d/d_c > 0.3$. In methane at $d/d_c > 1.0$, the value of $b_{GP}d$ increases rapidly. The increase is attributed to conduction-band formation and the associated decrease in the mean scattering cross section of the molecules for electrons. The implication is that the major part of the thermalization distance in the liquid phase is attained while the electron is inside the conduction band, within a few tenths of an eV of thermal energy. A similar conclusion was drawn earlier on theoretical grounds.[13] The nonspherelike ethane molecules do not permit formation of a smooth conduction band, so the spectacular increase of $b_{GP}d$ that occurs in methane does not occur in ethane (Fig. 4).

At $d/d_c > 1.5$, the thermalization distances decrease moderately in both liquids (Fig. 4). The decrease is attributed to stronger scattering by short-range interactions as the space between the molecules becomes small. In each liquid the decrease begins when the difference between the random—close-packed and van der Waals radii is reduced to 9×10^{-11} m. It might be a coincidence that these values are the same for a spherelike and nonspherelike molecular fluid.

The hump in $b_{GP}d$ in the density region $0.3 < d/d_c < 2.0$ corresponds to the "dense gas, low-density liquid" region of the coexistence fluids in which quasilocalization of thermal electrons occurs.[24,25,59–61] The hump in $b_{GP}d$ corresponds to a decrease in the average scattering cross section of the molecules for epithermal electrons, while quasilocalization is equivalent to an enhancement of the scattering of thermal electrons. Fluids in this intermediate density regime have relatively large density fluctuations that apparently influence the transport of thermal and epithermal electrons in opposite ways.

The final increase of $b_{GP}d$ in methane at its freezing point (Fig. 4) is due to the increased orderliness of the phase and consequent decrease of scattering. As an illustration of this effect, the value of $b_{GP}d$ in spherelike neopentane increased by 39% on going from the liquid at 258 K to the crystal at 253 K.[62] In methane, the 20% increase of $b_{GP}d$ between the points at the two highest densities (Fig. 4) might indicate that the last sample was partially frozen and should be plotted at a somewhat higher density than the liquid value shown. The analogous increase was not observed in ethane because the freezing point was not approached ($d_t/d_c = 3.2$, see Table I).

D. Correlation with electron mobility

There is a rough correlation between values of b_{GP} and thermal electron mobilities μ in a large series of liquids extending over six orders of magnitude of μ and two orders of magnitude of b_{GP}.[15] The correlation also exists for electrons in a given fluid at different densities, but there is a phase effect. The phase effect is dramatically illustrated by electron behavior in methane (Fig. 5).

In the gas phase the values of μ and b_{GP} each decrease approximately as d^{-1}, so a log-log plot of μ against b_{GP} for a gas at different densities has a slope of about unity (Fig. 5). In the denser gas, the curve, proceeding downward from the right, has a slightly steeper slope due to the more rapid decrease of μ caused by electron quasilocalization and the slightly less rapid decrease of b_{GP} illustrated in Fig. 4 as an increase in $b_{GP}d$. These are multibody effects. Upon increasing the density into the liquid phase, the direction of the methane curve reverses, with a large increase of μ and moderate increase of b_{GP} (Fig. 5). The curve is displaced upwards because thermal electrons ride near the bottom of the forming conduction band and are sensitive to the smoothness of it, whereas the secondary electrons ride above the band and then settle down

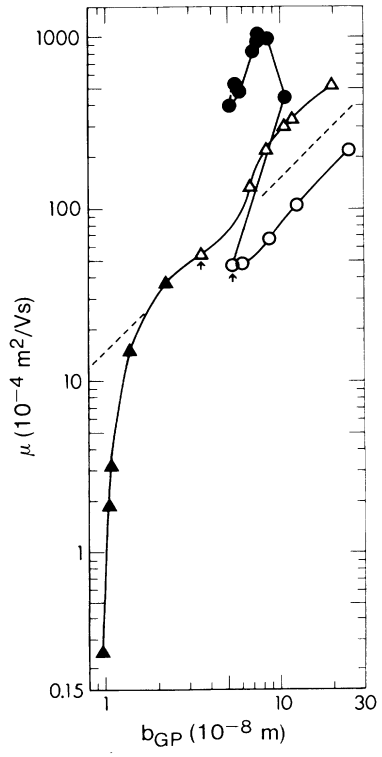

FIG. 5. Mobility μ of thermal electrons (Refs. 24 and 25) plotted against thermalization distance b_{GP} of secondary electrons in the coexistence vapor and liquid. Methane (circles), ethane (triangles); vapor (open points), liquid (closed points). The arrows mark the fluids at the critical density and near the critical temperature. — — —, arbitrary line with slope 1.0.

TABLE II. Summary of results.

T (K)	d (kg/m^3)	ϵ	G_{fi}^0	G_{tot}	b_{GP} (nm)	μ (10^{-4} m^2/V s) (Refs. 24 and 25)
			Methane			
91[a]	453	1.72	0.67	3.47	55	540
122	412	1.65	0.78	3.40	51	400
153	357	1.54	1.13	3.40	58	480
170	314	1.47	1.43	3.50	69	830
173	303	1.45	1.53	3.55	74	950
179	280	1.42	1.55	3.60	74	1040
180	276	1.41	1.68	3.55	84	980
188	220	1.31	1.64	3.08	107	510
192	162	1.22	0.83	2.74	53	47
190	119	1.16	0.99	3.10	60	48
183	77	1.09	1.34	3.30	86	66
173	46	1.05	1.75	3.57	123	109
158	23	1.03	2.62	4.00	248	236
144	12	1.02		3.80		440
			Ethane			
166	571	1.82	0.09	4.50	9.5	0.22
224	503	1.70	0.21	4.50	10.3	1.84
242	476	1.65	0.28	5.00	10.7	3.03
281	404	1.54	0.48	4.60	13.6	14.9
298	338	1.44	0.88	4.00	22.2	37
306	203	1.25	1.29	4.00	35	54
296	95	1.12	2.46	4.95	67	134
286	68	1.07	2.33	4.43	82	221
276	51	1.06	2.58	4.43	104	307
273	46	1.05	2.69	4.36	117	337
256	28	1.03	3.40	4.72	196	520

[a]This sample might have been partially frozen. The density and dielectric-constant values are those of the liquid.

through it as they undergo inelastic collisions. The more energetic electrons undergo harder collisions than do thermal electrons and experience less smoothing of the scattering potentials as the conduction band forms. Thus b_{GP} increases much less than does μ (Fig. 5).

As the density of liquid methane is increased from $d/d_c = 1.4$ to 2.5, the value of the electron thermalization distance decreases monotonically, while the thermal electron mobility passes through the familiar maximum at $d/d_c = 1.8$ (Ref. 24) (Fig. 5). The final reversal of direction of the curve between the last two points is due to the increased orderliness in the medium (decreased structure factor[62,63]); the relatively large effect observed with the present sample was possibly caused by partial crystallization, since the lowest temperature was the freezing point (Table II) and the recorded temperature could have been in error by a degree.

The plot of μ against b_{GP} for electrons in ethane is less complex than that for electrons in methane (Fig. 5). The differences between the two curves are attributed to the difference in degree of sphericity of the molecules and the shape effect on electron scattering. In the gas phase, electrons with energies <0.10 eV are scattered less strongly by less spherelike molecules.[61,64] Thermal electron (~ 0.03 eV) mobility is therefore larger in ethane than in methane gas at a given density, while the values of b_{GP} are similar in the two gases (Fig. 4). Thus, the curve in Fig. 5 for gas-phase ethane lies above that for methane. The increase of slope in the dense gas due to the decrease of μ by quasilocalization is more marked in ethane than in methane, because in the latter, the effect of quasilocalization is partially counteracted by the tendency to form a conduction band in the dense gas. In ethane the conduction band does not have a smooth bottom because orientational disorder of the rodlike molecules creates potential fluctuations which scatter the electrons. The formation of a conduction band on increasing the density into the liquid phase causes the slope of the ethane curve to decrease, but does not cause it to fold back as in methane (Fig. 5). At the highest densities, the value of μ in ethane plunges due to the formation of more stable localized states.[25] The value of b_{GP} reflects the behavior of higher energy electrons, above the localization levels, and is less affected by them. The lower end of the ethane curve in Fig. 5 therefore has a very steep slope.

ACKNOWLEDGMENTS

We would like to thank the Natural Sciences and Engineering Research Council of Canada for financial assistance, and the staff of the Radiation Research Center for aid with the electronics.

[1]G. R. Freeman, J. Chem. Phys. 39, 988 (1963); 39, 1580 (1963).
[2]P. H. Tewari and G. R. Freeman, J. Chem. Phys. 49, 954 (1968).
[3]P. H. Tewari and G. R. Freeman, J. Chem. Phys. 49, 4394 (1968).
[4]W. F. Schmidt and A. O. Allen, J. Phys. Chem. 72, 3730 (1968).
[5]P. H. Tewari and G. R. Freeman, J. Chem. Phys. 51, 1276 (1969).
[6]W. F. Schmidt and A. O. Allen, J. Chem. Phys. 52, 2345 (1970).
[7]K. Horacek and G. R. Freeman, J. Chem. Phys. 53, 4486 (1970).
[8]R. A. Holroyd, B. K. Dietrich, and H. A. Schwarz, J. Phys. Chem. 76, 3794 (1972).
[9]M. Nishkawa, Y. Yamaguichi, and K. Fujita, J. Chem. Phys. 61 2356 (1974).
[10]J. M. Warman and M. C. Sauer, Jr., J. Chem. Phys. 62, 1971 (1975).
[11]G. R. Freeman and J. M. Fayadh, J. Chem. Phys. 43, 86 (1965).
[12]A. Hummel, A. O. Allen, and F. H. Watson, Jr., J. Chem. Phys. 44, 3431 (1966).
[13]A. Mozumder and J. L. Magee, J. Chem. Phys. 47, 939 (1967).
[14]J.-P. Dodelet and G. R. Freeman, Can. J. Chem. 50, 2667 (1972).
[15]J.-P. Dodelet, K. Shinsaka, U. Kortsch, and G. R. Freeman, J. Chem. Phys. 59, 2376 (1973).
[16]J. L. Magee and W. P. Helman, J. Chem. Phys. 66, 310 (1977).
[17]J.-P. Dodelet, K. Shinsaka, and G. R. Freeman, Can. J. Chem. 54, 744 (1976).
[18]J.-P. Dodelet, Can. J. Chem. 55, 2050 (1977).
[19]J.-P. Dodelet and G. R. Freeman, Can. J. Chem. 55, 2264 (1977).
[20]T. G. Ryan and G. R. Freeman, J. Chem. Phys. 66, 5144 (1978).
[21]M. G. Robinson, P. G. Fuochi, and G. R. Freeman, Can. J. Chem. 49, 984 (1971).
[22]M. G. Robinson, P. G. Fuochi, and G. R. Freeman, Can. J. Chem. 49, 3657 (1971).
[23]M. G. Robinson and G. R. Freeman, Can. J. Chem. 52, 440 (1974).
[24]N. Gee and G. R. Freeman, Phys. Rev. A 20, 1152 (1979).
[25]N. Gee and G. R. Freeman, Phys. Rev. A 22, 301 (1980).
[26]J. W. T. Spinks and R. L. Woods, *An Introduction to Radiation Chemistry,* (Wiley-Interscience, New York, 1976), 2nd ed., Chaps. 2 and 3.
[27]U. Fano, in *Studies in Penetration of Charged Particles in Matter,* Natl. Acad. Sci.-N.R.C. Publ. 1133 (Natl. Acad. Sci.-N.R.C., Washington, D.C., 1964), pp. 311 and 312.
[28]R. M. Leblanc and J. A. Herman, J. Chem. Phys. 63, 1055 (1966); R. Cooper and R.-M. Mooring, Aust. J. Chem. 21, 2417 (1968).
[29]T. A. Stoneham, D. R. Ethridge, and G. G. Meisels, J. Chem. Phys. 54, 4054 (1971); B. Grosswendt and E. Waibel, Nucl. Instrum. Methods 155, 145 (1978).
[30]P. Langevin, C. R. Acad. Sci. (Paris) 134, 414 (1902).
[31]R. D. Goodwin, Natl. Bur. Stand. (U.S.) Tech. Note 653 (U.S. GPO, Washington, D.C. 1974).
[32]R. D. Goodwin, H. M. Roder, and G. C. Straty, Natl. Bur. Stand. (U.S.) Tech. Note 684 (U.S. GPO, Washington, D.C., 1976).
[33]L. N. Canjar and F. S. Manning, *Thermodynamics and Reduced Correlations for Gases* (Gulf Publishing, Houston, 1967).
[34]N. E. Hill, W. E. Vaughan, A. H. Price, and M. Davies, *Dielectric Properties and Molecular Behavior* (Van Nostrand Reinhold, Toronto, 1969), p. 191.
[35]J. R. Partington, *An Advanced Treatise on Physical Chemistry* (Longmans, London, 1954), Vol. 5, p. 349.
[36]*Handbook of Chemistry and Physics,* edited by R. C. Weast (Chemical Rubber Co., Cleveland, Ohio, 1969), 50th ed.
[37]L. Onsager, Phys. Rev. 54, 554 (1938).
[38]F. M. Jacobsen, N. Gee, and G. R. Freeman, in *Positron Annihilation,* edited by P. G. Coleman, S. C. Sharma, and L. M. Diana (North-Holland, Amsterdam, 1982), p. 92.
[39]Y. Toi, D. B. Peterson, and M. Burton, Radiat. Res. 17, 399 (1962).
[40]H. H. Carmichael, P. Gordon, Jr., and P. Ausloos, J. Chem. Phys. 42, 343 (1965).
[41]M. Trachtman, J. Phys. Chem. 70, 3382 (1966).
[42]K. H. Jones, J. Phys. Chem. 71, 709 (1967).
[43]W. J. Beekman, Physica (Utrecht) 15, 327 (1949); A. Ore and A. Larson, Radiat. Res. 21, 331 (1964).
[44]J.-P. Dodelet and G. R. Freeman, Int. J. Radiat. Phys. Chem. 7, 183 (1975).
[45]G. R. Freeman, in *The Study of Fast Processes and Transient Species by Electron Pulse Radiolysis,* edited by J. H. Baxendale and F. Busi (Reidel, Dordrecht, 1982), pp. 21–23; J. Chem. Phys. 46, 2822 (1967), App. B.
[46]J. Terlecki and J. Fiutak, Int. J. Radiat. Phys. Chem. 4, 469 (1972).
[47]G. R. Freeman and J.-P. Dodelet, Int. J. Radiat. Phys. Chem. 5, 371 (1973).
[48]J.-P. Dodelet and G. R. Freeman, Can. J. Chem. 49, 2643 (1971); 50, 2729 (1972).
[49]G. C. Abell and K. Funabashi, J. Chem. Phys. 58, 1079 (1973).
[50]A. Mozumder, J. Chem. Phys. 60, 4305 (1974).
[51]J.-P. Dodelet and G. R. Freeman, J. Chem. Phys. 60, 4657 (1974).
[52]J. Casanovas, R. Grob, D. Blanc, G. Brunet, and J. Mathieu, J. Chem. Phys. 53, 3673 (1975).
[53]M. Baba and K. Fueki, Bull. Chem. Soc. Jpn. 48, 2240 (1975).
[54]D. S. Sethi, H. T. Choi, and C. L. Braun, Chem. Phys, Lett. 74, 223 (1980).
[55]H. T. Choi, D. S. Sethi, and C. L. Braun, J. Chem. Phys. 77, 6027 (1982).
[56]G. R. Freeman and T. E. M. Sambrook, J. Phys. Chem. 78, 102 (1974).
[57]S. S.-S. Huang and G. R. Freeman, Can. J. Chem. 55, 1838 (1977).
[58]M. G. Robinson and G. R. Freeman, J. Chem. Phys. 55, 5644 (1971).
[59]S. S.-S. Huang and G. R. Freeman, J. Chem. Phys. 68, 1355 (1978).
[60]S. S.-S. Huang and G. R. Freeman, Phys. Rev. A 24, 714 (1981).
[61]N. Gee and G. R. Freeman, J. Chem. Phys. 78, 1951 (1983).
[62]K. Shinsaka and G. R. Freeman, Can. J. Chem. 52, 3556 (1974).
[63]J. Lekner and A. R. Bishop, Philos. Mag. 27, 297 (1973).
[64]G. R. Freeman, I. György, and S. S.-S. Huang, Can. J. Chem. 57, 2626 (1979).